GLOBAL TOPOGRAPHY OF DIONE: EFFECTS OF LARGE IMPACTS ON GLOBAL SHAPE. P. Schenk[1], W. B. McKinnon[2], J. M. Moore[3], [1]Lunar & Planetary Institute/USRA, Houston TX (schenk@lpi.usra.edu). [2]Dept. EPSC and McDonnell Center for Space Sci., Washington University in St. Louis, Saint Louis, MO 63130, [3]NASA Ames Research Center, Moffett Field, CA 94035.

Introduction: Saturn's icy moon Dione has been extensively resurfaced and is second only to Enceladus in terms of geologic complexity [1]. Dione may thus represent a fossil version of that active moon. It is also currently in a 2:1 mean-motion orbital resonance with Enceladus and is experiencing modestly enhanced heating (possibly greater in the past). Like Enceladus, Cassini acquired global stereo imaging of Dione. Here we report on construction of an updated global DEM, with emphasis on global properties, influence of large impacts on that shape, and comparisons with Enceladus.

Topographic Mapping of Dione: To produce a global topographic map of Dione (Fig. 1) referenced to the limb-derived triaxial shape of the body [2] we use the same approach used for our high resolution global topographic map of Enceladus [3, 4]. Using ISIS tools, we first register the complete Dione image library using match points and solve for the camera pointing vectors of those images using bundle adjustment, simultaneous solving for match point radii relative to the center of the body. Stereogrammetric digital elevation models (DEMs) are then produced, with each DEM mapped to the global match point radius map. The result is a high-resolution global map of elevations on Dione relative to the triaxial figure (Fig. 1); produced at a base resolution of 400 m. Weakest stereo coverage is south of 60°S, where imaging resolutions were > 750 m/pixel.

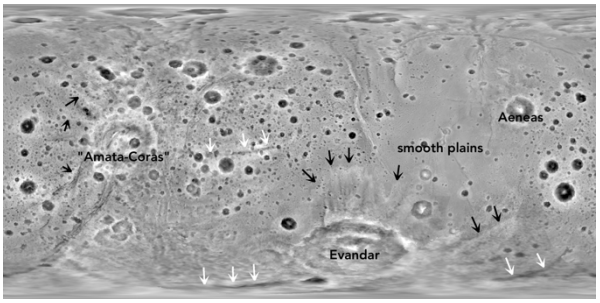

Figure 1. Global DEM of Dione in cylindrical projection, centered on the anti-Saturn point. Vertical scale shown is -3.5 to +2.5 km. Major basins are labeled; radial features and ejecta are highlighted by arrows. Leading hemisphere is on the right, trailing on the left.

Global Topographic Characteristics: Relief across Dione is very low, with ~95% of all terrains being less than 1.5 km above or below the local triaxial surface. This range of relief is second only to Enceladus among Saturn's icy moons in terms of narrowness [1], and even then, most of the extremes in relief are due to the 50-100 km craters, the deepest of which are 3-4 km.

Dione lacks the 100-km scale >1 km deep topographic depressions evident on Enceladus [3,4]. These large 'dimples' can be attributed to thickness variations in the ice shell, possibly due to ongoing internal activity, but density variations may also play a role. Spherical harmonic analysis of the new global DEMs of both satellites confirms the visual impression that Dione lacks Enceladus' strong degree-3 latitudinal shape distortion [4-6] inferred to result from the geologic activity at Enceladus' south polar terrains. Either Dione's ice shell was too thick [5] to distort in these ways or any signature of such past activity relaxed away once Dione's elevated heat flow [7] declined substantially. Our Dione solution is referenced to and is a good match to the triaxial solution of [2], which however, itself possesses excess flattening [5]. Dione may about 100 m more rotationally flattened than in [2], but this is well within the 1-σ uncertainty of the limb solution [5,6].

Large Impact Effects on Dione: The absence of a significant topographic signature from internal mass (re)distribution at low degrees greater than 2 on Dione leaves large impact as the dominant topographic signature. Moore et al. [8] previewed possible geologic effects of large impact prior to Cassini. The global elevation map confirms there are only 3 recognizable impact features >150 km on Dione (and only 4 between 100 and 150 km), much fewer than observed on Iapetus [1,9]. The generally low relief (inferred by [1] to be due to extensive icy plains volcanism) allows topographic effects of large basins to be identified without interference from the signatures of dense cratering.

Pancake ejecta is common around 40-100-km craters on smooth plains. Ejecta is also evident in low-Sun images of Aeneas crater (D~160 km), a standard albeit partially relaxed central peak crater [7], but the limits of such deposits are not well mapped due to degradation.

The two largest features are Evander basin and a prominent ringed feature at 5°N, 74°E named here Amata-Coras for two prominent peak craters located within it. Evander (60°S, 214°E) is ~335 km across and has a peak/peak ring morphology (Fig. 2, top), with a prominent 4-km-high central peak surrounded by a 2/3rd complete peak ring ~180 km in diameter. This morphology is unusual for large basins on these satellites, with

most >250 km basins having a conic central peak morphology [1]; only 320-km relaxed Telamus on Tethys also has the complex peak/peak ring morphology.

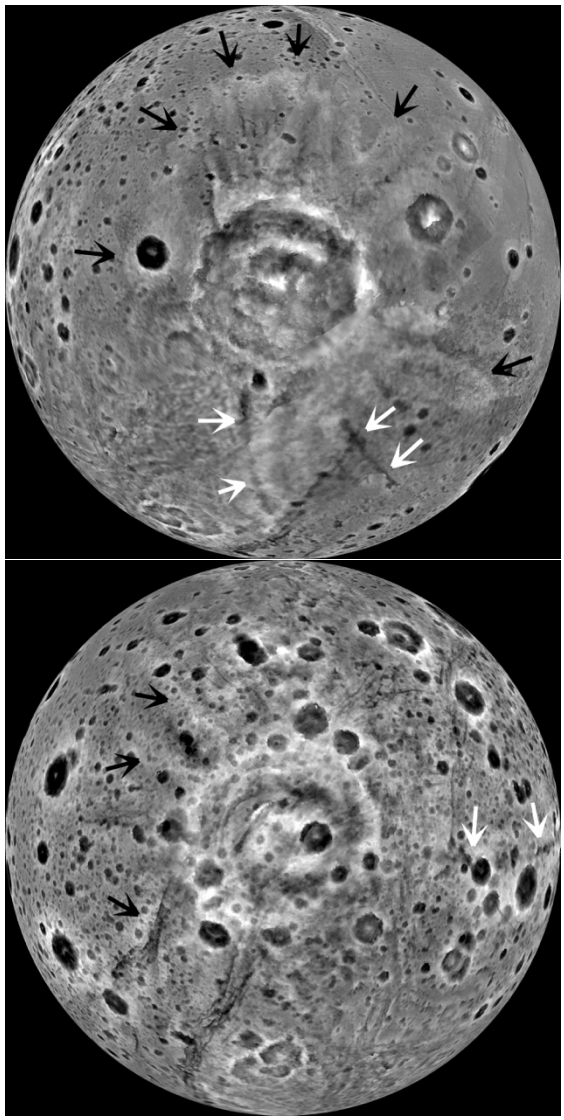

Figure 2. Orthographic hemispheric views of global DEM centered on Evander (top) and the Amata-Coras ring basin (bottom). Black arrows indicate distal ejecta ridges at Evander and radial features at Amata-Coras. White arrows indicate radial troughs. Vertical scale shown is -2.5 to +2.5 km.

A discreet ejecta unit surrounds most of Evander, with the outer margin forming a prominent ridge 1-2 km high. This morphology resembles single-layered ejecta units on Mars [10], though in this case the ridge could be ascribed to accumulation of debris at a decelerating flow front. The outer margin of this deposit forms at distances of ~125 to 300 km from the basin rim, where identifiable. In the more extended portions of the deposit several radial striations are observed. Both the distal ridge and radial striations are prominent features to the east of 400-km-wide Odysseus basin on Tethys, which were also interpreted as ejecta deposits by [1]. Despite the prominence of these features, they do not form extended plateaus surrounding either basin.

The Amata-Coras ringed feature (Fig. 2, bottom) is a prominent oval double ring structure ~325x385 km wide. This older degraded feature still retains a prominent double ring structure. Although no distal ejecta ridge is evident due to this degradation, several cryptic radial structures are evident to the west, some of these mimic azimuthal ejecta thickness variations at Evander (Fig. 2) and could be remnant ejecta effects. Post Amata-Coras graben-like fractures follow or are strongly influenced by Amata-Coras ring contours as well as radial topographic features to the west.

Other features include several prominent 400-km radial grooves that curve outward from the rim of Evander, and a single 500-km-long radial groove curves outward from Amata-Coras (Fig. 2). Whether these radial grooves are secondary crater chains or large fractures is not evident, but, at both basins, these grooves curve significantly to the left as viewed from the rim.

The topographic expression of the two large basins on Dione is complex. Relief of 3-4 km is observed on the rim scarps and the central peaks or peak rings of both. The mean elevations across both when the topography of each is summed, is only a few hundred meters, indicating both are strongly relaxed (either during or post-impact), consistent with evidence of widespread relaxation and elevated heat flow from smaller craters [7]. The lack of deep volume deficits at either basin indicates that any basin mass anomalies that might trigger polar wander [11] are not very large.

Our topographic mapping of Dione confirms it has low global relief and lacks the pronounced distortion signatures of Enceladus. Global effects of large impact include variable ejecta deposits up to 1 km thick and radial troughs. Topographic signatures of older large basins on Dione have been (nearly) completely erased.

References: [1] Schenk et al., (2018) in *Enceladus*, Univ. Arizona Press. [2] Thomas, P., (2010) *Icarus*, 208, 395-401. [3] Schenk, P., and W. McKinnon (2009), *GRL*, 36, L16202. [4] Schenk, P., and W. McKinnon (2020), *AGU*, P001-04; in preparation. [5] Zannoni M. et al. (2020) *Icarus 345*, 113713. [6] Nimmo, F., et al. (2011) *JGR*, 116, E11001. [7] White, O., et al., (2017) *Icarus*, 288, 37-52. [8] Moore, J. et al. (2004), *Icarus*, 171, 421-443. [9] Kirchoff, M. et al. (2018) in *Enceladus*, Univ. Arizona Press. [10] Barlow, N. (2006) *MAPS*, 41, 1425-1436. [11] Nimmo, F. and I. Matsuyama (2007) *GRL*, 34, L19203.